Y. Fang[1], X. Wang[1,2,3], J. Ren[3,4], H. Liu[3,4] and Y. Wang[3,5]

[1] School of Geography and Planning, Sun Yat-sen University, Guangzhou 510275, China

[2] Guangdong Provincial Engineering Research Center for Public Security and Disasters, Guangzhou 510275, China

[3] Southern Marine Science and Engineering Guangdong Laboratory (Zhuhai), Zhuhai 519082, China

[4] School of Marine Sciences, Sun Yat-sen University, Zhuhai 519082, China

[5] School of Earth Sciences and Engineering, Sun Yat-sen University, Zhuhai 519082, China

Corresponding authors:

Xianwei Wang (wangxw8@mail.sysu.edu.cn)

Jie Ren (renjie@mail.sysu.edu.cn)

Key Points:

- Elucidate the mechanism of flood diversion between West River and North River at an H-shaped SXJ node.
- Quantify the influence of flood diversion on discharge and peak water levels in downstream branches.
- Reveal critical flow ratios for incoming flow without diversion and discharge rates after flood diversion.

Abstract

Most studies focus on flow division at a Y-shaped river bifurcation, while few studies investigate flood diversion at an H-shaped river node. The Delft3D model is built to simulate the flood diversion and discharge division at the H-shaped SiXianJiao (SXJ) node in the northwestern apex of the Pearl River Delta (PRD), South China, based on three flood events and 121 combinations of upstream flow rates. Results showed that the H-shaped SXJ node created an unstable state due to unbalanced upstream flood waves, while always approaching equilibrium by flood diversion through the SXJ waterway. There exists a critical flow ratio of 75.9% that the incoming flow from both rivers poses a similar water level at both river mouths, resulting in near equilibrium and little flood diversion. Above the threshold, the flood water will divert from West River to North River with a maximum rate of -10700 m^3/s, reducing the peak water level up to 1.48 m at Makou. Below the threshold, the flood water will divert from North River to West River with a maximum rate of 11900 m^3/s, reducing the peak water level up to 6.63 m at Sanshui. Meanwhile, the discharge ratio at the downstream Makou and Sanshui approaches a stable value during individual flood and fluctuates around a critical value of 76.6%. This critical discharge ratio is consistent with those observed during the flood events in 2005 (77.2%),

2006 (76.8%) and 2022 (75.9%), and confirms the empirical relation adopted in calculating the design flood stages in the PRD.

Key Words: Discharge division; Flood diversion; H-shaped node; Unstable equilibrium; Water level changes

Plain Language Summary

The SiXianJiao (SXJ) waterway connects West River and North River at the H-shaped SXJ node in the Pearl River Delta (PRD), South China. We established the Delft3D model to simulate the flood diversion using three floods and 121 combinations of flow rates. Results show that the flood diversion is driven by the water level differences at both river mouths. We discovered a critical flow ratio of 75.9% at Gaoyao, which poses a similar water level at both river mouths, resulting in near equilibrium and little flood diversion. Above the threshold, it will divert the flood water from West River to North River with a maximum rate of -10700 m^3/s, reducing the peak water level up to 1.48 m at Makou. Below the threshold, it will divert the flood water from North River to West River with a maximum rate of 11900 m^3/s, reducing the peak water level up to 6.63 m at Sanshui. The discharge ratio at the downstream Makou and Sanshui approaches a stable value during individual flood events and fluctuates around a critical value of 76.6%. Such a critical discharge ratio was also observed during the flood events in 2005 (77.2%), 2006 (76.8%) and 2022 (75.9%).

1 Introduction

The Pearl River delta (PRD) has a complicated river network and offers an opportunity to study the flow and sediment distribution at various bifurcations (Zhang et al., 2014). Divisions of flow and sediment at bifurcations in the PRD have been changing over the past half century, resulting in varying ratios of flow and sediment draining into the South China Sea through the eight outlets (Luo et al., 2007). The SiXianJiao (SXJ) node located in the northwestern apex of the PRD controls the division of flow and sediments from the upstream West River and North River into the downstream river network, eventually affecting the estuary development and the flood risk along the downstream waterways (Xie et al., 2010; Zhang et al., 2017).

The SXJ node was in X-shape, where the flow confluence and division occurred simultaneously and water exchanged freely for West River and North River over a thousand years ago (Zeng and Huang, 1982; Ying et al., 1988; Wu and Wei, 2021). With aggradation of sediment and human embankment, West River and North River had been separated and are connected by a 3-km length waterway at present (Liu, 2014), forming a unique H-shaped node with varying and asymmetrical double bifurcations (Figure 1), where once flow division occurs in West River, flow confluence happens in North River, vice versa. The H-shaped river node created an unstable equilibrium modulated by flow diversion due to different ratios of upstream inflow and asynchronous tide in downstream branches (Zhang et al., 2014; Wu, 2018). Most previous studies focused on flow and sediment division at regular Y-shaped bifurcations (Wang et al., 1995; Bertoldi,

2004; Kleinhans et al., 2007, 2008, 2013; Buschman et al., 2010; Schurrman et al., 2015), while few studies investigated how the flow diversion and discharge division occurred at an X-shaped river node with free water (mass) exchange (Ying et al., 1988; Ferguson et al., 1992) , or at an H-shaped river node with double bifurcations and constrained water (mass) exchange (Shen, 1989; Liu, 2008; Li, 2018).

Figure 1. Satellite image of Sixianjiao (a) and a simplified H-shaped river node (b). Gaoyao and Shijiao are the two control stations in the upstream, and Makou and Sanshui are the two control stations in the downstream. Q_a and Q_b represent the incoming flow at Gaoyao from West River and at Shijiao from North River. Q_c and Q_d represent the discharge rates at Makou and Sanshui in the downstream branches. Q_x is the diversion flow via the SXJ waterway.

River bifurcations distribute water, sediment and, indirectly, flood risk over the downstream river branches (Kleinhans et al., 2008). At regular Y-shaped river bifurcations where the geometry of the upstream river and the two downstream branches are symmetrical, the distribution of water over the two downstream branches is mainly controlled by the channel dimensions and hydraulic roughness (Wang et al., 1995). Most river bifurcations are asymmetrical (Bolla Pittaluga et al., 2003). Such asymmetries include different channel directions, bending, width and depths with respect to the upstream river channel and the downstream branches (Ramamurthy et al., 2007). Asymmetrical bifurcations are always unstable because of the erodible banks and river bed and a larger share of flow and sediment developed in one of the downstream branches (Buschman et al., 2010). Even symmetrical river bifurcations always turn into asymmetrical in allocating flow and sediment after decades to centuries, depending on integrated effects of various factors, including regional factors and local

factors (Kleinhans et al., 2007). Regional factors are external boundary conditions in the upstream feeding river and the downstream branches. Local factors are internal features such as bar and meander dynamics (Kleinhans et al., 2008). When a bifurcation is affected by tides in coastal river deltas like the SXJ node, the flow and sediment distribution becomes more complicated and is not well understood (Buschman et al., 2010; Ji and Zhang, 2019).

The discharge ratio at the SXJ node has been greatly altered in past decades (Wu et al., 2018). The discharge ratio at Makou of the downstream West River branch was about 78%~90% (average 82%) of total flow from the upstream West River and North River before early 1990s, while it had decreased to 73%~80% (average 75%) since 1990s (Liu and Wu, 2005; Zhang et al., 2014; Liu et al., 2019). Accordingly, the discharge rate at Sanshui of the downstream North River branch almost doubled (Xie et al., 2010; Wang et al., 2015). Liu (2016) analyzed the variation characteristics of flow division at the SXJ node by constructing a numerical network model under various incoming flow rates and at different tidal levels of estuary. Ji and Zhang (2019) employed a two-dimensional hydrodynamic model to study the subtidal discharge division in the entire PRD and discussed the sensitivity of the discharge division to incoming fresh flow and tides. However, these studies did not investigate how the flow diversion via the SXJ waterway influences the discharge ratios.

The flow diversion in the SXJ waterway was indirectly estimated by an approach of water balance using flow measurements at two upstream stations (Gaoyao and Shijiao) and two downstream stations (Makou and Sanshui) illustrated in Figure 1. Consistent with the discharge ratio change at Makou and Sanshui, the estimated annual diversion via the SXJ waterway flowed from North River to West River before 1992, and have been reversed since 1993 (Liu, 2008). Shen (1989) established a numerical model based on the residuals of water balance at the upstream and downstream flow stations to estimate the flow diversion, which was comparable to the *in situ* flow measurement in the SXJ waterway in low-water periods (Jan, Fen and Mar) from 1961 to 1964. Nonetheless, the flow diversion in the low-water period was mainly controlled by the asynchronous tides in the downstream branches (Zhang et al., 2018), and the application of such statistic model that ignored the tidal force was limited in a changing environment. Li (2018) constructed a stage-discharge relation in the SXJ waterway by multivariate linear regression using *in situ* measurements during a flood period in 2017. In the model, the water level difference at stations between Ganggen in the middle of SXJ waterway and Makou/Sanshui in the downstream branches was used to fit the flood diversion for the first time, which is close to reveal the driving force of flood diversion. The estimated peak diversion rate (-6050 m^3/s) was quite similar with the observed flow (-6100 m^3/s). The largest diversion flow (-6930 m^3/s) in the SXJ waterway was observed on July 22, 1996, which reduced the peak water levels in the West River at Makou by 0.96 m and at Gaoyao by 0.79 m (Li, 1997).

The SXJ waterway plays a crucial role on redistributing flood water from the

upstream West River and North River and greatly mitigates the flood risk in the downstream branches. However, there is lack of studies to investigate the diversion mechanism and the influence of flood diversion on the downstream river network. The primary aim of this study is to investigate the hydrodynamic characteristics of the flood diversion via the SXJ waterway at the H-shaped SXJ node, and to quantify how flood diversion influences the discharge ratio and peak water levels at the downstream Makou and Sanshui based on historical flood events and various flood scenarios simulated by a 2D hydraulic model. Session 2 describes the study area and data, session 3 explains the model setup and scenario modeling, session 4 presents the results, followed by discussion in session 5 and conclusion.

2 Study Area and Data

This session describes the study area, various data resources and the stage-flow curves at Makou and Sanshui from historical flood events.

2.1 Study Area

The PRD in South China consists of the eastern delta fed by East River and the northwestern delta fed by West River and North River (Figure 2). The annual mean stream flow of West River, North River and East River are 7124 m^3/s, 1465 m^3/s and 719 m^3/s (Zhang et al., 2018). The SXJ node is at the northwestern apex of the PRD and has a drainage area 399 830 km^2, of which those above Gaoyao in West River and Shijiao in North River are 351 535 km^2 (99% of the West River basin) and 38 363 km^2 (86% of the North River basin), respectively (Liu, 2008). Gaoyo and Shijiao are 45 km and 52 km away from the SXJ waterway, and are the control stations of West River and North River. The SXJ is the first exchange node via the SXJ waterway for West River and North River and controls the flow and sediment distribution in the downstream branches. The SXJ waterway is near 3 km length from the west mouth to the east mouth, and 200 to 500 m wide at water levels of 1.0 to 10 m at the narrower west mouth. The mean depth of the SXJ waterway is -15 m with two deeper pools near the west mouth (-30 m) and north mouth (- 20 m), between which there is a relatively shallower session of river bed with 10-m depth (Figure 2).

The PRD has complex river networks. Makou and Sanshui are the two control stations after both rivers enter the PRD. Makou is 4 km downstream away from the west mouth, while Sanshui is near 1 km away from the east mouth. The discharge in the downstream West River and North River is further diverted into the river network at the second and third bifurcation nodes, and finally pours into the South China Sea through the eight outlets, i.e., Humen, Jiaomen, Hongqimen, Hengmen, Modaomen, Jitimen, Hutiaomen, and Yamen (Figure 2).

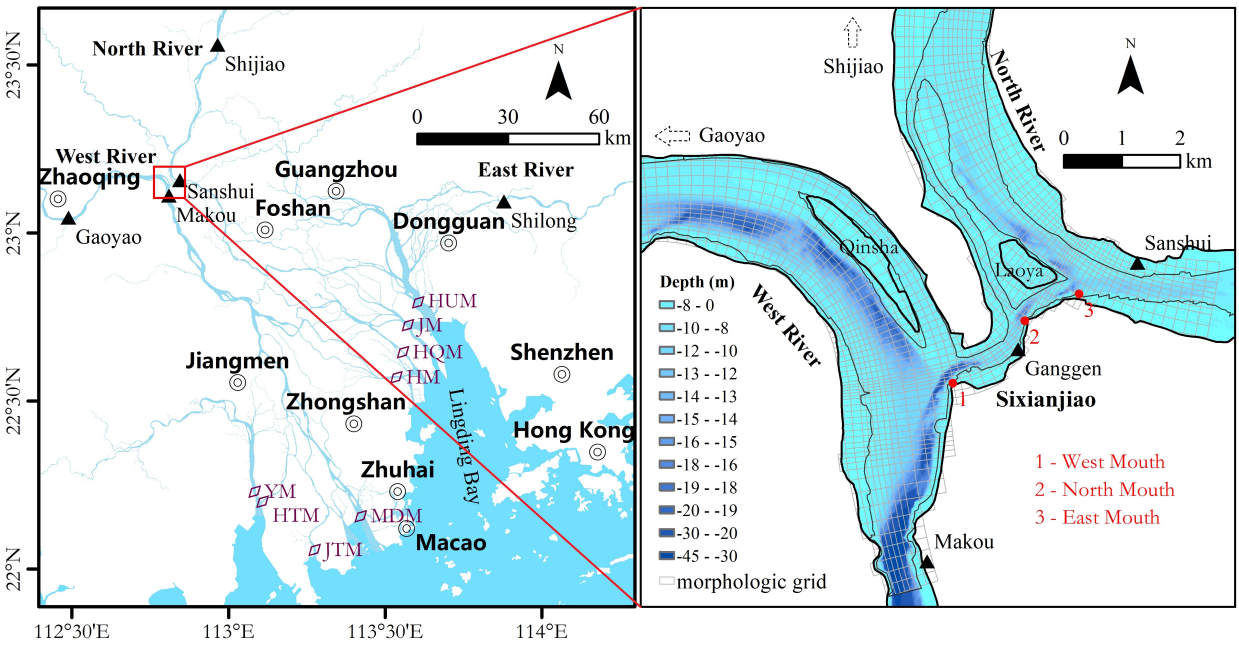

Figure 2. The SXJ node in the PRD. The right plot is a part of the model grid over the SXJ node. The abbreviations are the eight outlets, Humen (HUM), Jiaomen (JM), Hongqimen (HQM), Hengmen (HM), Modaomen (MDM), Jitimen (JTM), Hutiaomen (HTM), Yamen (YM). The filled red circles in the SXJ waterway are the junctions, called west mouth, north mouth, and east mouth, where water levels are used to analyze the flood diversion via the SXJ waterway.

2.2 Data Description

The data used in this study are summarized in Table 1. The bathymetry data of the SXJ node were surveyed in 2020 by the Pearl River Hydraulic Research Institute of Pearl River Water Resources Commission of Ministry of Water Resources (MWR) and converted into a 5 m grid. The water level and discharge were obtained from Pearl River Hydraulic Research Institute and Department Water Resources (DWR) of Guangdong Province. The water level and flow recorded during the flood events in 2005, 2006, 2017 and 2022 at Gaoyao, Shijiao, Makou and Sanshui were used to calibrate and validate the model, and to analyze the flood diversions via the SXJ waterway.

The design flood flow at Gaoyao and Shijiao stations were officially issued by the DWR of Guangdong Province in 2002 and were used to set the upstream boundary condition for scenario simulation (DWR, 2002). The flow varies from 37900 to 57500 m^3/s at Gaoyao and from 11900 to 20700 m^3/s at Feilaixia/Shijiao, representing the extreme flow for return periods from 5 to 300 years (Table 2). All elevation and water level data were converted to the 1985 Yellow Sea Geodatum in this study.

Table 1. Description and sources of data used to model flood discharges in SXJ of Guangdong Province

Item	Description	Source
Bathymetry	Precision: 0.1 m;	Pearl River Hydraulic Research Institute o
Water level and flow	Hourly, Gaoyao, Shijiao, Makou, Sanshui	Pearl River Hydraulic Research Institute o

Note. MWR-Ministry of Water Resources; DWR-Department of Water Resources

Table 2. The flood flow and return periods at Gaoyao from West River and Feilaixia/Shijiao from North River (DWR, 2002)

River/Stations	Return periods (1: n year) and flow (m^3/s)					
	5	10	20	30	50	100
West River/Gaoyao	37900	45000	49700	50800	52200	54000
North River/Feilaixia	11900	13800	15500	16700	16700	17700

Note. Feilaixia is located 40 km upstream of Shijiao

2.3 Historical Floods and Stage-Flow Curves

The 2005 flood event occurred from June 4 to July 9, and were dominated by West River. The peak flow reached 56 300 m^3/s at Gaoyao and 13 500 m^3/s at Shijiao, which represent a frequency of near 0.5% (200a return periods) and 10% (10a return periods), respectively. The flood water was mainly diverted from West River to North River via the SXJ Waterway. The peak flood levels at Makou and Sanshui reached 9.71 m.

The magnitude of the 2006 flood was much smaller than that in 2005. The peak water level reached 6.6 m at Makou and Sanshui, and the peak flow at Gaoyao and Shijiao reached 32000 m^3/s and 17500 m^3/s, respectively, and were equivalent to a 5-year flood in West River and a 50-year flood in North River. The flood water was mainly diverted from North River to West River.

In order to set flexible boundary conditions in downstream, the stage-flow curves at Makou and Sanshui were fitted by a quadratic polynomial with the stage and flow data during the flood events of 2005 and 2006 in Equations (1) and (2):

$$Q_{\mathrm{mk}} = 254.33Z_{\mathrm{mk}}^2 + 2654.2Z_{\mathrm{mk}} + 8106.7 \quad (1)$$

$$Q_{\mathrm{ss}} = 49.325Z_{\mathrm{ss}}^2 + 1095.6Z_{\mathrm{ss}} + 1990.9 \quad (2)$$

where Z_{mk} and Z_{ss} are the water levels (m), and Q_{mk} and Q_{ss} are flow (m^3/s) at Makou and Sanshui.

The correlation coefficients between flow and water levels reached 0.99 at Makou and Sanshui (Figure 3a&b). Both fitted equations were relatively stable and could well estimate the flood flow with water levels recorded during the flood occurred in June 2022, having R^2 by 0.96 and 0.98, and Mean Absolute Difference (MAD) by 1830 m^3/s at Makou and 432 m^3/s at Sanshui (not shown).

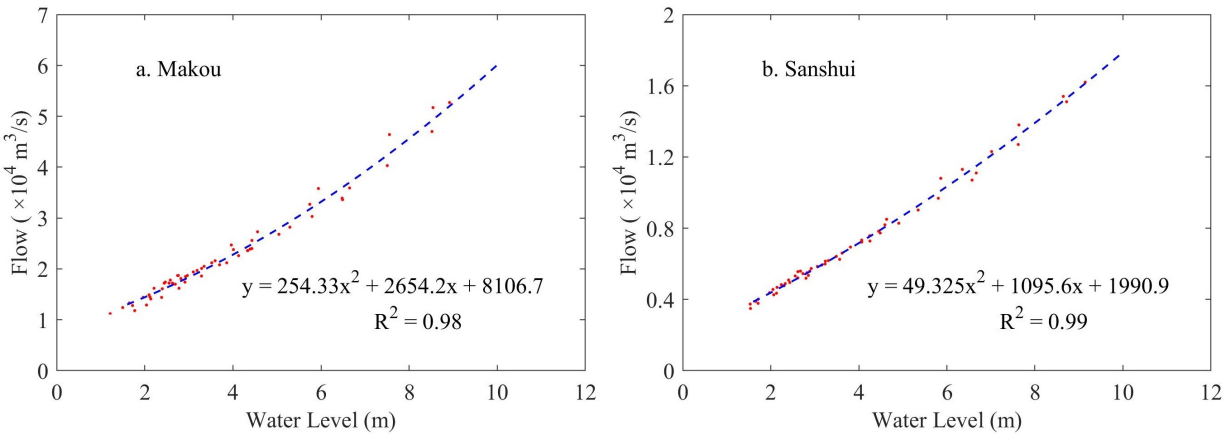

Figure 3. The Stage-flow curves at Makou (a) and Sanshui (b) fitted by the flow and water levels recorded during the 2005 and 2006 flood events.

3 Barotropic Modeling of Flow

The methodology session consists of three parts, i.e. the model setup, model calibration and validation using historical flood events, and scenario simulations with total 121 combinations of incoming flood flow from West River and North River.

3.1 Model Setup

The Delft3D model was established with Cartesian grids at the SXJ node using the bathymetry data, which contain the levee height and river bed/beach elevation (Deltares, 2018). The river banks were constrained by the levees. The model consists of 302 and 45 grid points in the M and N direction, respectively. There are overall 14, 9 and 8 grid cells with varying sizes across West River, North River and the SXJ waterway. Some local areas are widened to keep the boundary in line with the river banks. The simulation domain starts at the upstream Gaoyao in West River and Shijiao in North River and ends at the downstream Makou in West River branch and Sanshui in North River branch. The upstream boundary conditions were set with streamflow at Gaoyao and Shijiao, and the downstream boundary stations at Makou and Sanshui were not set with flow or water level, but with their flexible stage-flow curves fitted in Figure 3. The flow was simulated using the depth-averaged 2D shallow water equations, which solves the unsteady shallow water equations, since the depth-averaged 2D simulations were comparable to those by the 3D simulations in

several coastal cases (Lesser et al., 2004; Deltares, 2018).

3.2 Model Calibration and Validation

The Delft3D model was calibrated using the measured flow and water levels from 4 June to 10 July 2005. The upstream boundary conditions were the measured streamflow at Gaoyao and Shijiao. The initial water level was set for that on 4 June 2005 at Makou. The initial Manning's roughness coefficients followed the recommended values in the user manual, varying from 0 to 0.04 (Deltares, 2018). The Nash-Sutcliffe efficiency coefficient (NSE) and MAD between the simulated and observed water levels and discharge at Makou and Sanshui were used to optimize the model parameters. The NSE and MAD were computed using Eq. 3 and Eq. 4, respectively (Nash and Sutcliffe, 1970; Pinos and Timbe, 2019).

$$NSE = \mathrm{NSE} = 1 - \frac{\sum(X_{\mathrm{obs}} - X_{\mathrm{mod}})^2}{\sum(X_{\mathrm{obs}} - \overline{X}_{\mathrm{obs}})^2} \quad (3)$$

$$\mathrm{MAD} = \frac{1}{N}\sum_{i=1}^{N} |X_{\mathrm{obs}} - X_{\mathrm{mod}}| \quad (4)$$

where X_{obs} is observation for water level or discharge, X_{mod} is simulation, is $\overline{X}_{\mathrm{obs}}$the mean value of observations. The performance levels of the model are classified excellent fit for NSE > 0.65, very good fit for $0.5 <$ NSE < 0.65, good fit for $0.5 <$ NSE < 0.5, poor fit for NSE < 0.2 (Allen et al., 2007; Maréchal, 2004).

The model was validated using the recorded flood data at the four stations of Gaoyao, Shijiao, Makou and Sanshui from June 5 to June 30, 2022. By keeping the other parameters unchanged, only the upstream flow at Gaoyao and Shijiao were replaced. The water level and discharge at Makou and Sanshui were used to validate the simulated values.

3.3 Scenario Simulations

A series of model runs were conducted with total 121 combinations for the upstream boundary conditions of steady flow (Table 3) based on the design flood flow issued by Department of Water Resources of Guangdong Province in 2002 (Table 2). The incoming flow varies from 10000 m^3/s to 60000 m^3/s with an interval of 5000 m^3/s at Gaoyao in West River and from 2000 m^3/s to 22000 m^3/s with an interval of 2000 m^3/s at Shijiao in North River. The downstream boundary conditions were set with the stage-flow curves in Equations (1) at Makou and Equations (2) at Sanshui, instead of specific flow or water levels. The bed roughness is set as a uniform Manning value of 0.035 $m^{-1/3}s$ in all runs. A time step of 3 seconds was used to keep the steady flow stable.

Table 3. The upstream boundary conditions of incoming flow at Gaoyao from West River and Shijiao from North River for scenario simulations.

Rivers/Stations	Flow (m^3/s)									
West River/ Gaoyao	10000	15000	20000	25000	30000	35000	40000	45000	50000	550

Rivers/Stations	Flow (m^3/s)									
North River/ Shijiao	2000	4000	6000	8000	10000	12000	14000	16000	18000	200

4 Results

The session presents the results for model calibration and validation, three typical flood events simulations, and scenario simulations for 121 combinations of incoming flood flow from West River and North River.

4.1 Model Calibration and Validation

For the model calibration, the simulated water levels and discharge agreed well with the *in situ* observations at Makou and Sanshui during the 2005 flood (Figure 4). The NSEs of water levels and discharge are 0.99 at Makou and Sanshui, and the MADs of water levels and discharge are 0.19 m and 0.14 m, 1262 m^3/s and 425 m^3/s, respectively. The relative differences (RMAD) of the simulated discharge against the mean flow were 5.2% and 5.6%.

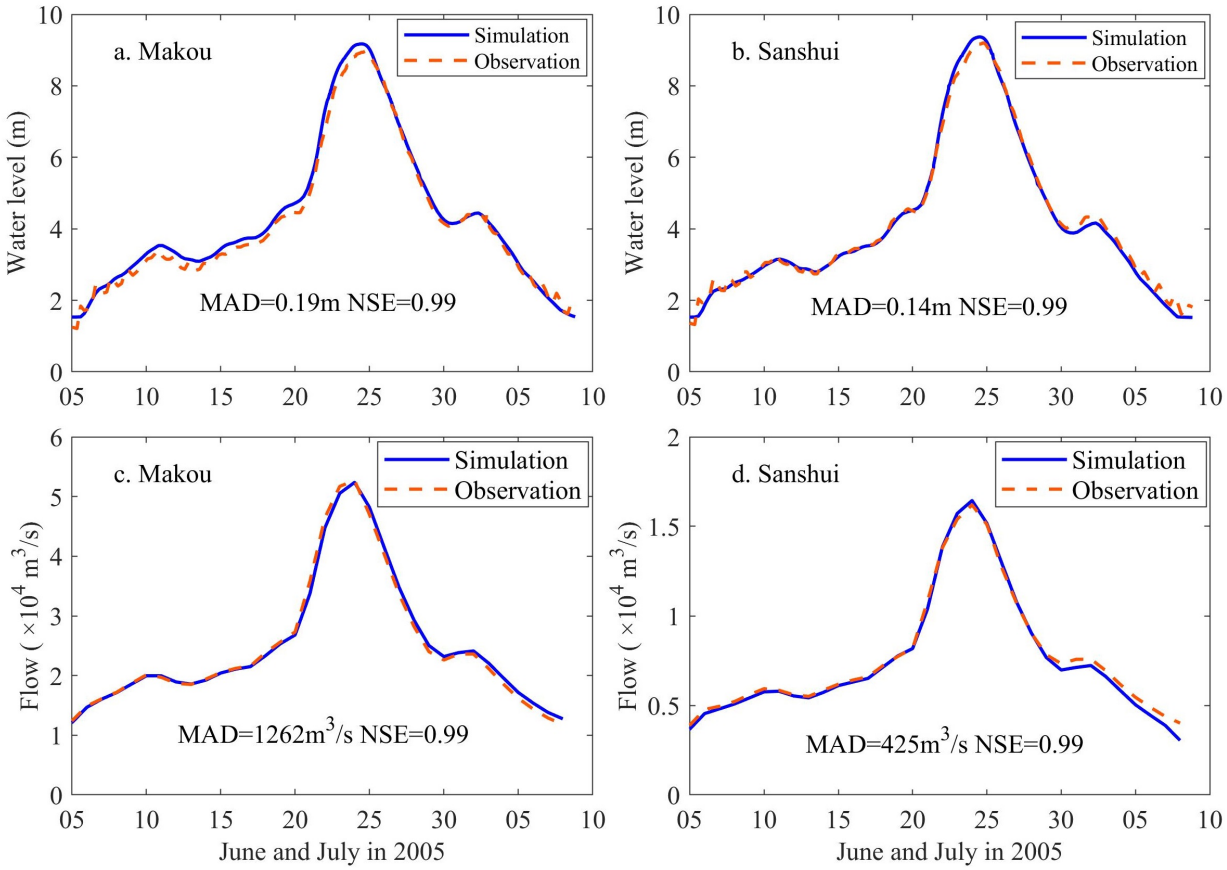

Figure 4. Model calibration of water levels (a, b) and discharge (c, d) using *in situ* measurements at Makou (a, c) and Sanshui (b, d) during the flood from June 5 to July 10, 2005.

For the model validation, the simulated water levels and discharge during the 2022 flood matched well with *in situ* observations. The NSEs of water levels and discharge are 0.94 and 0.97, 0.96 and 0.93 at Makou and Sanshui, and the MADs are 0.26 m and 0.17 m, 983 m^3/s (RMAD=2.8%) and 627 m^3/s (RMAD=5.8%), respectively (Figure 5). During the 2017 flood, the discharge at Makou (NSE=0.97, MAD= 956 m^3/s, RMAD=3.9%) and Sanshui (NSE=0.98, MAD= 262 m^3/s, RMAD=3.6%) were also successfully simulated (Figure 6), and the simulated diversion flow via the SXJ waterway was in agreement with the *in situ* observations by NSE of 0.87 and MAD of 385 m^3/s (RMAD=13.9%).

The above results for model calibration and validation indicate that the Delft3D model can be used to simulate the flood diversion and discharges at the SXJ node under different scenarios of incoming flood flow from West River and North River.

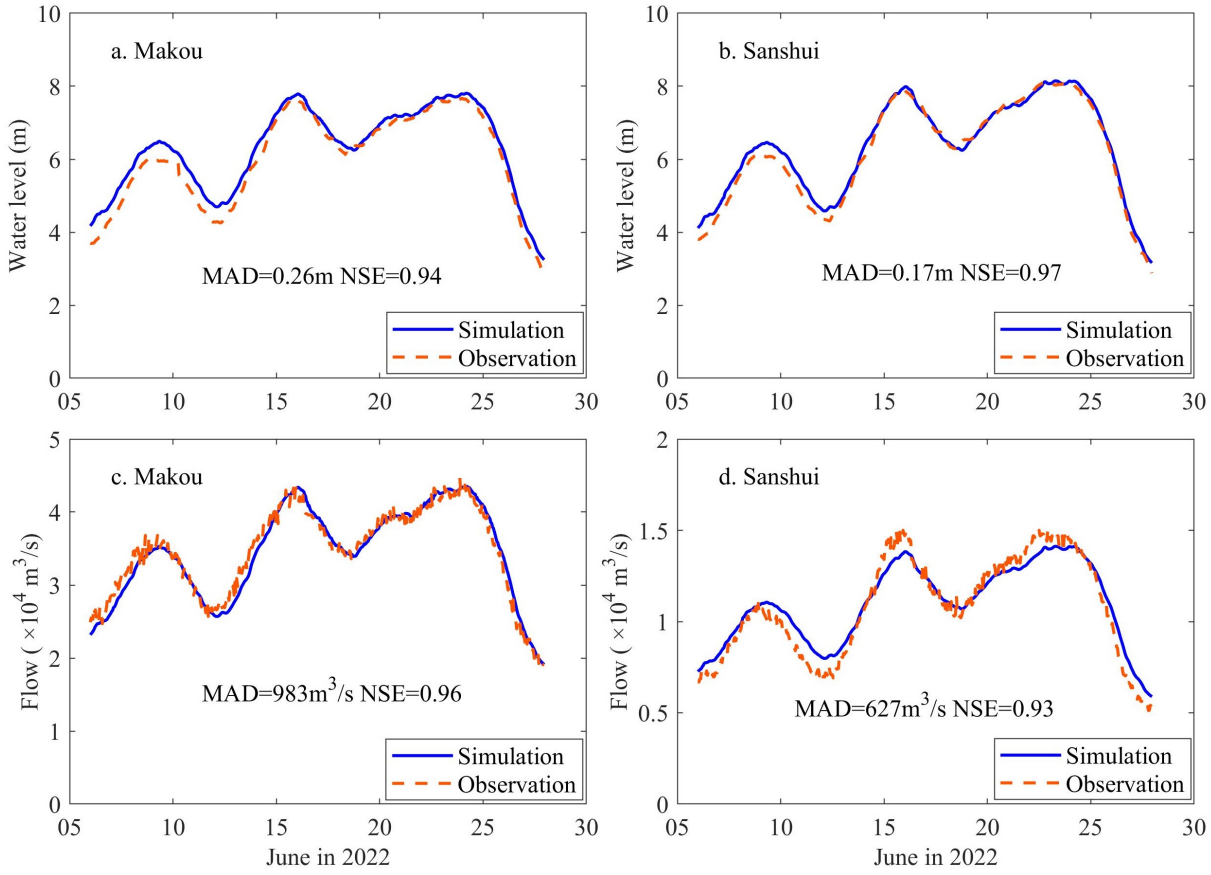

Figure 5. Model validation of water levels (a, b) and discharge (c, d) using *in situ* measurements at Makou (a, c) and Sanshui (b, d) during the flood from June 5 to June 27, 2022.

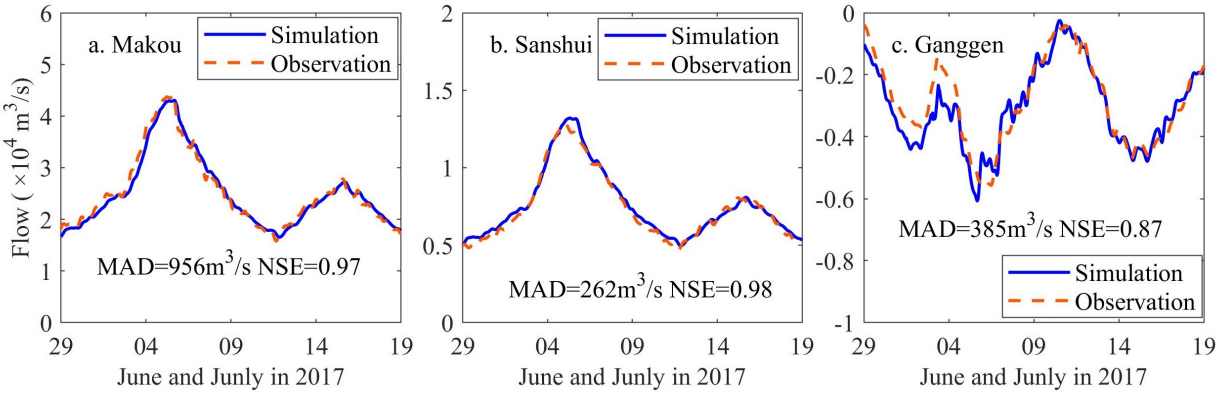

Figure 6. Model validation using *in situ* flow observation at Makou, Sanshui and Ganggen during the flood from June 29 to July 19, 2017.

4.2 Flood Event Simulation

Three typical flood events in 2005 (single flood wave), 2006 (two and three flood waves in North River and West River) and 2022 (three flood waves) were simulated to illustrate the flood diversion effects by the SXJ waterway under different incoming flood waves at Gaoyao from West River and at Shijiao from North River (Figures 7-9).

4.2.1 Flood event in 2005

The flood event occurred in 2005 was dominated by a single flood wave from West River (Figure 7a), where the incoming flow ratio at Gaoyao (Gaoyao / [Gaoyao + Shijiao]) varied from 80% to 93% from June 10 to July 5 (Figure 7b). Accordingly, the water levels at the west mouth of the SXJ waterway were 4 to 23 cm higher than its north mouth, resulting in flood diversion from West River to North River via the SXJ waterway with a peak flow of -5630 m^3/s (Figure 7c). Here the positive flow was defined as it flows from North River to West River following the historical flow diversion status (Liu, 2008). With flood diversion, the discharge ratios at Makou (Makou / [Makou+Sanshui]) and Sanshui were quite stable through the event, around 77.2% and 22.8%, respectively (Figure 7b). The return periods of peak flow were 1:200a at Gaoyao from West River and 1:10a at Shijiao from North River, and changed to 1:60a and 1:30a after flood diversion (Table 4). Without flood diversion, the water levels at Makou would increase by 0.7m (Figure 7d), i.e., flood diversion reduced the peak water level at Makou up to 0.7 m, and the peak flow reduced from 56667 m^3/s (1:200a) to 52601 m^3/s (1:60a) (Table 4). The average rate of flow diversion during the flood from June 5 to July 10 was -2512 m^3/s (West -> North), or total volume

by -7.6 km^3, which was over half of the annual mean total water diversion (-14.2 km^3) from 1993 to 2005 (Liu, 2008).

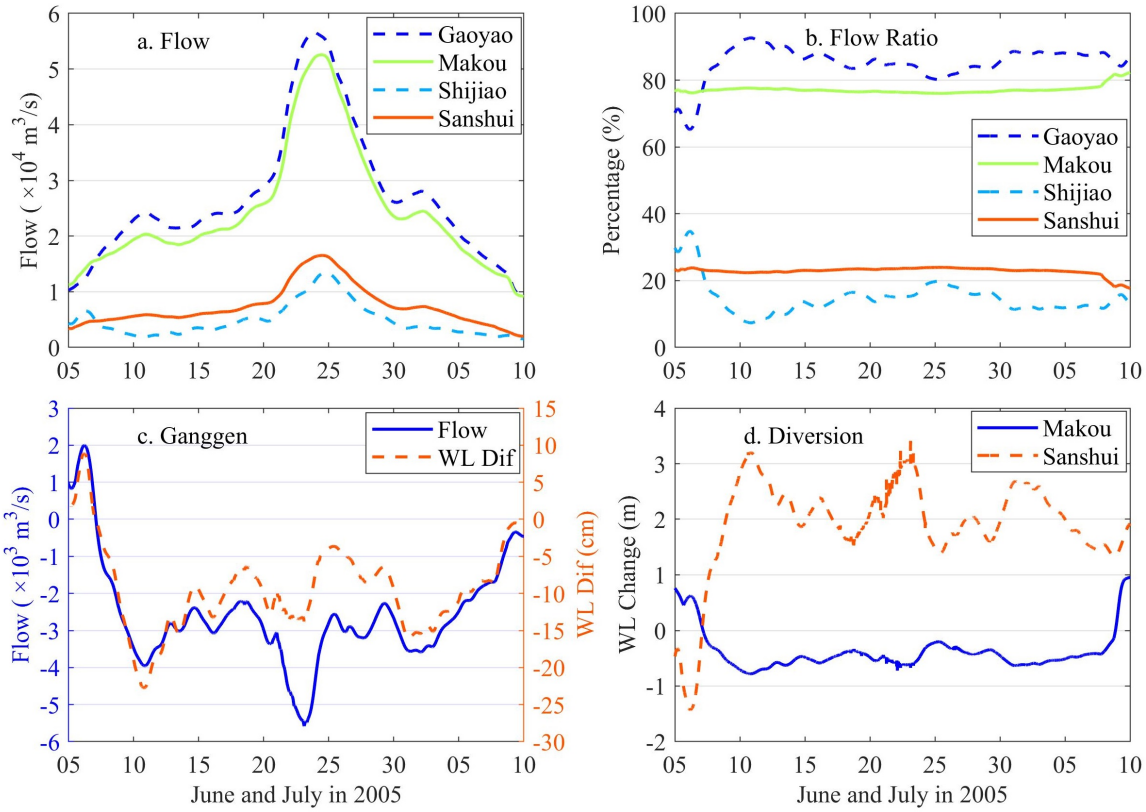

Figure 7. The simulated flow and water levels at the SXJ node during the 2005 flood. The incoming and outgoing flow (a) and flow ratio (b) of West River and North River, (c) the diversion flow at Ganggen and water level difference (N-W) between north mouth and west mouth of the SXJ waterway, and (d) water level changes with and without flood diversion, which was calculated as the actual water levels with flood diversion minus the given water levels without flood diversion that the discharge at Makou (Sanshui) is same as the incoming flow at Gaoyao (Shijiao) from West River (North River).

Table 4. Comparisons of peak flow at Gaoyao (Shijiao) and discharge at Makou (Sanshui) in West (North) River after flood diversion via the SXJ waterway.

Flood Events /Phases	Upstream Stations	Peak Flow (m^3/s)	Return Periods (a)	*Flow Ratio	Downs
2005 Flood	Gaoyao	56667	200	80.9%	Makou
	Shijiao	13400	10	19.1%	Sanshu
2006 Flood	Gaoyao	34435	2	65.4%	Makou
	Shijiao	18245	60	34.6%	Sanshu

Flood Events /Phases	Upstream Stations	Peak Flow (m^3/s)	Return Periods (a)	*Flow Ratio	Downs
2022 Flood I	Gaoyao	37366	5	78.7%	Makou
	Shijiao	10109	2	21.3%	Sanshu
2022 Flood II	Gaoyao	42415	10	73.4%	Makou
	Shijiao	15372	20	26.6%	Sanshu
2022 Flood III	Gaoyao	39381	5	66.6%	Makou
	Shijiao	19768	100	33.4%	Sanshu

Note: *Flow (discharge) ratio is the percentage of total incoming flow (discharge). #The return periods at Makou (Sanshui) were assessed with the flow frequency distribution function at Gaoyao (Shijiao) and approximated to the nearby values.

4.2.2 Flood event in 2006

The flood event in July 2006 consisted of three flood waves in West River and two waves in North River (Figure 8a), and the flood diversion in the SXJ waterway was alternatively controlled by the incoming flow from West River and North River and was divided into four phases (Figure 8d). The return periods of peak flow at Gaoyao and Shijiao were 1:2a and 1:60a, and changed to near 1:5a after flood diversion (Table 4). In phase I from July 11 to 16, the incoming flow was dominated by West River at Gaoyao, whose flow ratio varied around 94% (Figure 8b), and the peak water level at the north mouth of the SXJ waterway was 28 cm lower than its west mouth, resulting in peak flood diversion by -4000 m^3/s from West River to North River (Figure 8c), the peak water level reduction by 0.83 m at Makou and increase by 3.29 m at Sanshui (Figure 8d).

In phase II from July 16 to 20, the water levels at the SXJ node were dominated by the incoming flow from North River at Shijiao, whose maximum flow ratio increased from 7% to 42%, while it decreased from 94% to 58% at Gaoyao from West River (Figure 8b). The peak water level at the northern mouth of the SXJ waterway was 29 cm higher than its western mouth, resulting in peak flood diversion by 6300 m^3/s from North River to West River (Figure 8c), peak water level reduction by 3.35 m at Sanshui and increase by 1.34 m at Makou (Figure 8d). The peak flow rate (return periods) reduced from 18245 m^3/s (1:60a) to 12166 m^3/s (1:5a) at Sanshui (Table 4).

In phase III from July 20 to 27, the flood flow from North River retreated much faster than that from West River, and the incoming flow was dominated by West River at Gaoyao, whose flow ratio increased from 58% to 91% while it decreased from 42% to 9% at Shijiao. The peak water level at the north mouth of the SXJ waterway was 24 cm lower than its west mouth, resulting in peak flood diversion by -4600 m^3/s from West River to North River (Figure 8c), peak water level reduction by 0.75 m at Makou and increase by 3.4 m at Sanshui (Figure 8d).

In phase IV from July 27 to 31, the water levels at the SXJ node were dominated again by the flood wave from North River at Shijiao, whose maximum flow

ratio increased from 9% to 40%, while it decreased from 91% to 60% at Gaoyao (Figure 8b). The peak water level at the north mouth of the SXJ waterway was 18 cm higher than its west mouth, resulting in peak flood diversion by 3300 m^3/s from North River to West River (Figure 8c), peak water level reduction by 2.2 m at Sanshui and increase by 0.9 m at Makou (Figure 8d). With flood diversion, the discharge ratios at Makou and Sanshui were quite stable, around 76.8% and 23.2%, respectively (Figure7b). The average diversion rate during the flood from July 11 to 31 was -448 m^3/s (West -> North).

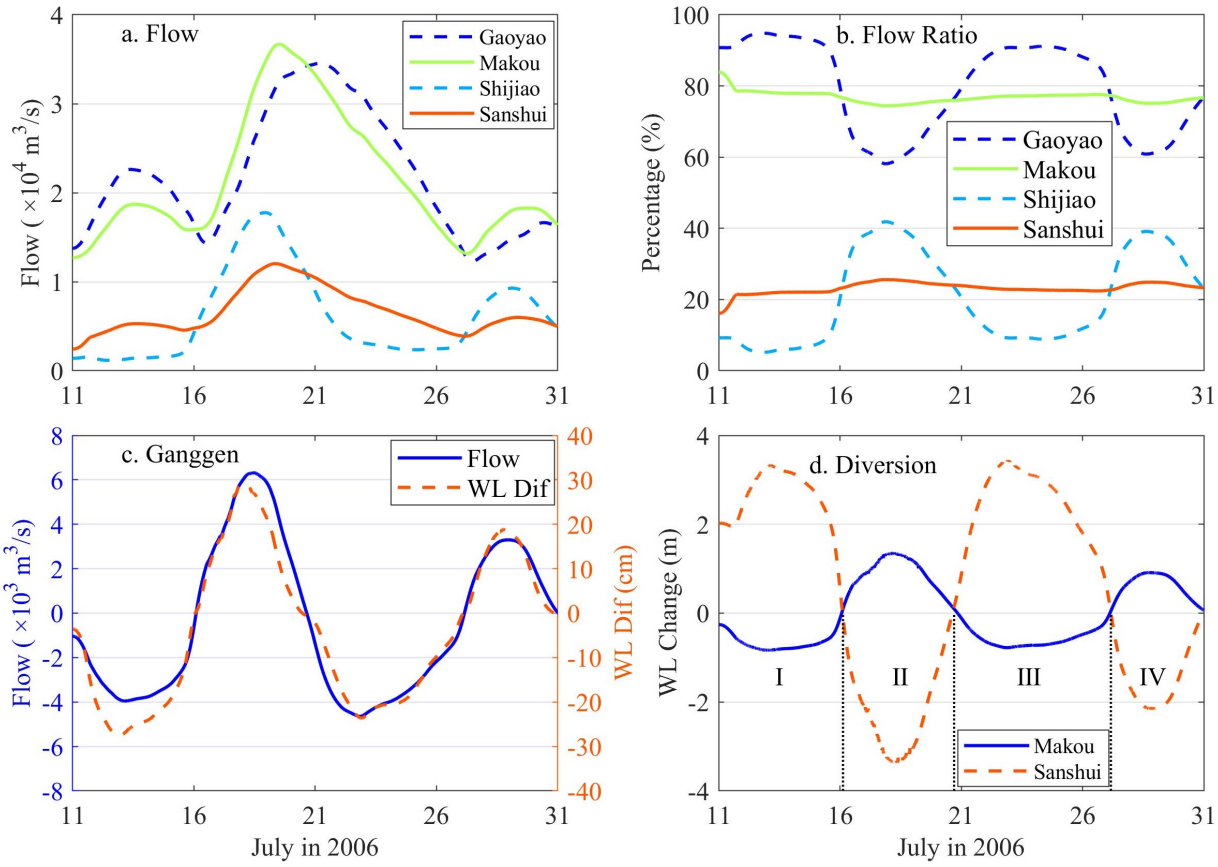

Figure 8. Same as figure 7 but for the 2006 flood.

4.2.3 Flood event in 2022

The flood event in 2022 consisted of three flood waves in both rivers (Figure 9a), and the flood diversion in the SXJ waterway were alternatively controlled by the incoming flow from West River and North River and were divided into three phases (Figure 9d). In phase I from June 5 to 14, the water levels at the SXJ node was dominated by the incoming flow from West River at Gaoyao, whose flow ratio varied around 81% (Figure 9b), and the peak water level at the noth

mouth of the SXJ waterway was near 5 cm lower than its west mouth, resulting in peak flood diversion by -2100 m^3/s from West River to North River (Figure 9c), peak water level reduction by 0.30 m at Makou and increase by 1.46 m at Sanshui (Figure 9d).

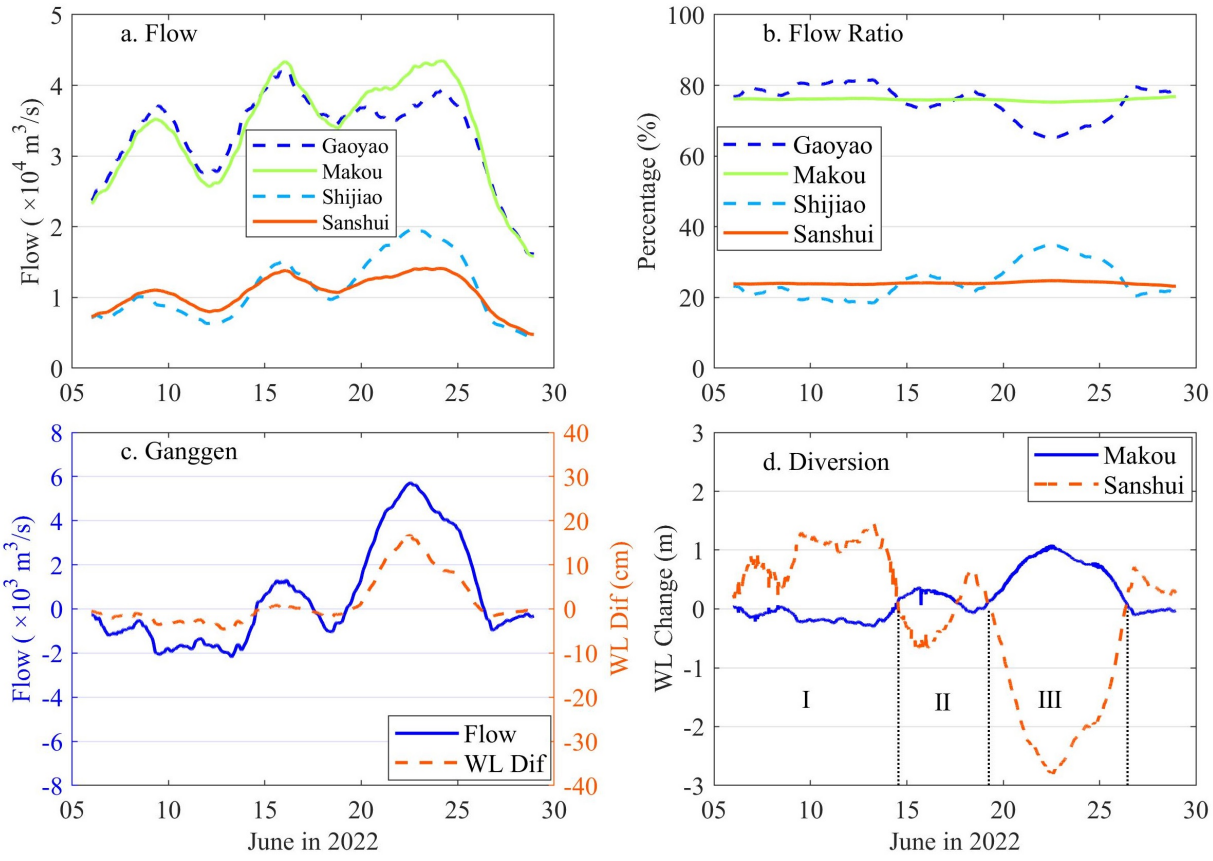

Figure 9. Same as figure 7 but for the 2022 flood.

In phase II from June 14 to 19, the averages of incoming flow ratio at Gaoyao from West River and at Shijiao from North River were 75.6% and 24.4% (Figure 9b), respectively, which posed a near equilibrium state with similar water levels at the north and west mouths of the SXJ waterway (Figure 9c). The flood diversion switched direction three times and had an average flow rate only by 217 m^3/s (Figure 9c).

In phase III from June 19 to 26, the water levels at the SXJ node was dominated by the incoming flow from North River at Shijiao, whose maximum flow ratio increased from 24% to 35%, while it decreased from 76% to 65% at Gaoyao (Figure 9b). The peak water level at the north mouth of the SXJ waterway was 16 cm higher than its west mouth, resulting in peak flood diversion by 5700

m^3/s from North River to West River (Figure 9c) and peak water level reduction at Sanshui by 2.8 m, while the peak water level at Makou increased by 1.1 m due to flood diversion (Figure 8d). With flood diversion, the discharge ratios at Makou and Sanshui were quite stable, around 75.9% and 24.1%, respectively (Figure 9b), and the return periods of peak flow at Shijiao reduced from 1:100a to 1:10a (Table 4). The average rate of flow diversion during the flood from June 5 to 30 was 574 m^3/s (North ->West).

In summary, the SXJ waterway played a significant role on diverting the flood water from both West River and North River. The diversion rate was controlled by the water level difference at the west and north mouths of the SXJ waterway and by the amount of relative incoming flow from West River and North River. The event-mean diversion rates were -2512 m^3/s (West -> North) in 2005, -448 m^3/s (West -> North) in 2006, and 574 m^3/s (North ->West) in 2022. Surprisingly, with flood diversion, the discharge ratio at the downstream Makou and Sanshui remained near stable during those floods. The discharge division at Sanshui (Makou) in 2022 (24.1%) showed a larger (smaller) value than those in 2006 (23.2%) and 2005 (22.8%) partly due to the relatively larger magnitude of peak flood in North River.

4.3 Flood Scenario Simulation

A total 121 combinations of steady flow representing various upstream flow conditions were run to simulate the flood diversion and discharge division at the SXJ node (Table 3 and Figure 10). The flood diversion was driven by the water level difference between the west and north mouth of the SXJ waterway, at which the water levels were determined by the incoming flow from West River and North River (Figure 10a). Under different incoming flow rates, a flow percentage threshold of 75.9% (Gaoyao / [Gaoyao + Shijiao]) exists when there is a common flood over 20 000 m^3/s at Gaoyao from West River (Figure 11a). Above this threshold, the water level at the north mouth is lower than the west mouth (Figure 10a), and the flood water will divert from West River to North River (W->N) with a maximum flow rate of -10700 m^3/s (Figure 10b), reducing the peak water level up to 1.48 m at Makou and escalating the peak water level up to 8.02 m at Sanshui (Figure 10c). Below this threshold, the water level at the north mouth is higher than its west mouth (Figure10a), and the flood water will divert from North River to West River (N->W) with a maximum flow rate of 11900 m^3/s (Figure 10b), reducing the peak water level up to 6.63 m at Sanshui and escalating the peak water level up to 2.95 m at Makou (Figure 10c). After the flood diversion, the division ratio of discharge at Makou (Makou / [Makou + Sanshui]) varies from 74.3% to 77.6% (Figure 10d). Even under different incoming flow rates from both rivers, the discharge ratios at Makou (or Sanshui) retain relatively stable during a flood and vary around a mean value of 76.6% when the discharge rate (water level) at Makou is over 20 000 m^3/s (3.0 m), when the tidal force on flow diversion turns secondary (Figure 11b).

The SXJ waterway plays a crucial role on diverting the flood water from either North River or West River and significantly reduces the peak water levels at

Makou and Sanshui (Figure 12). The diversion flow is over 53% of the North River flow and can reduce the peak water level up to 6.63 m at Sanshui. In contrast, it is just 20% of the West River flow and reduces the peak water level by 1.48 m at Makou (Figure 10b&c).

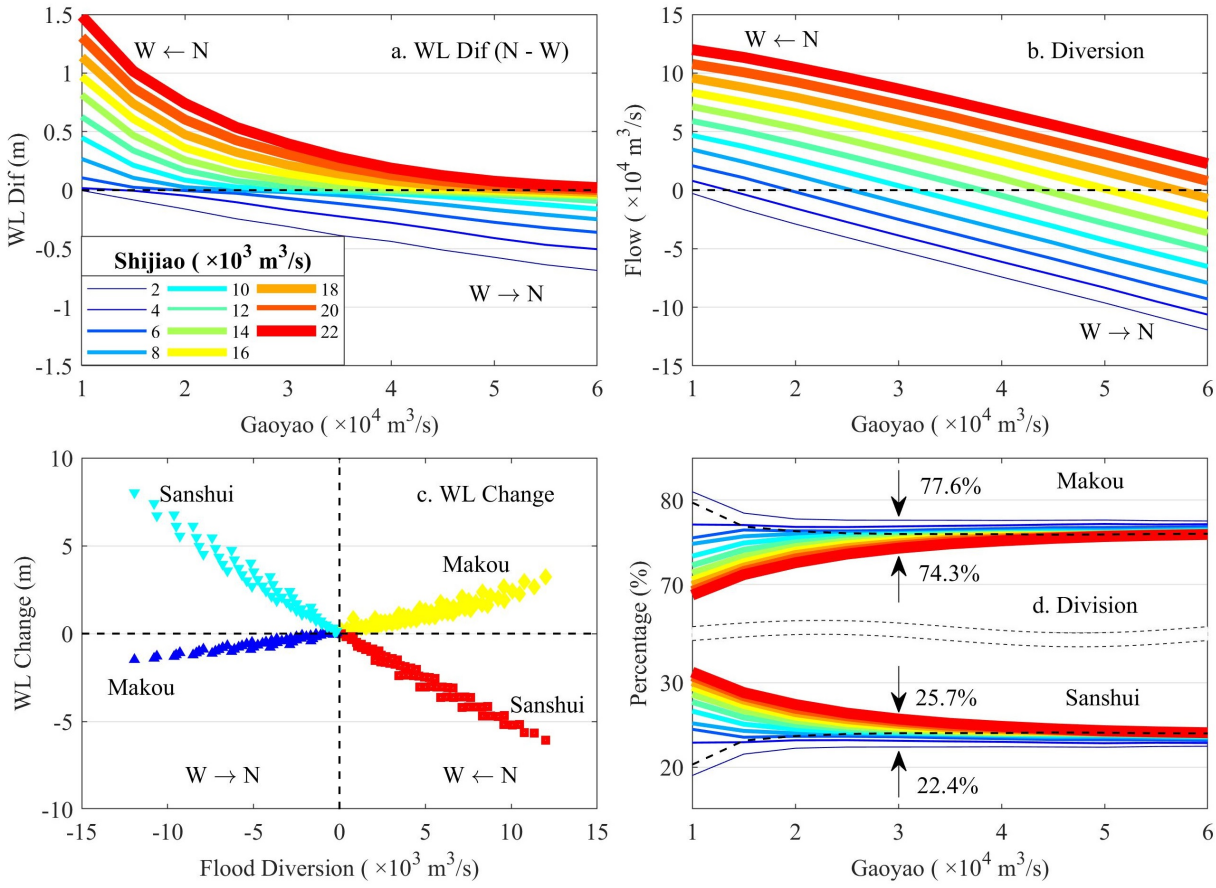

Figure 10. The flood diversion and discharge division simulated under various combinations of incoming flow at the SXJ node: (a) water level difference (N-W) between the north mouth and west mouth in the SXJ waterway, (b) flood diversion rate at Ganggen, (c) water level change with flood diversion, and (d) discharge division ratio at Makou and Sanshui in the downstream. In plot (d), the two arrows and values represent the upper and lower division ratio, and the dashed lines represent the incoming (discharge) flow ratio without flood diversion.

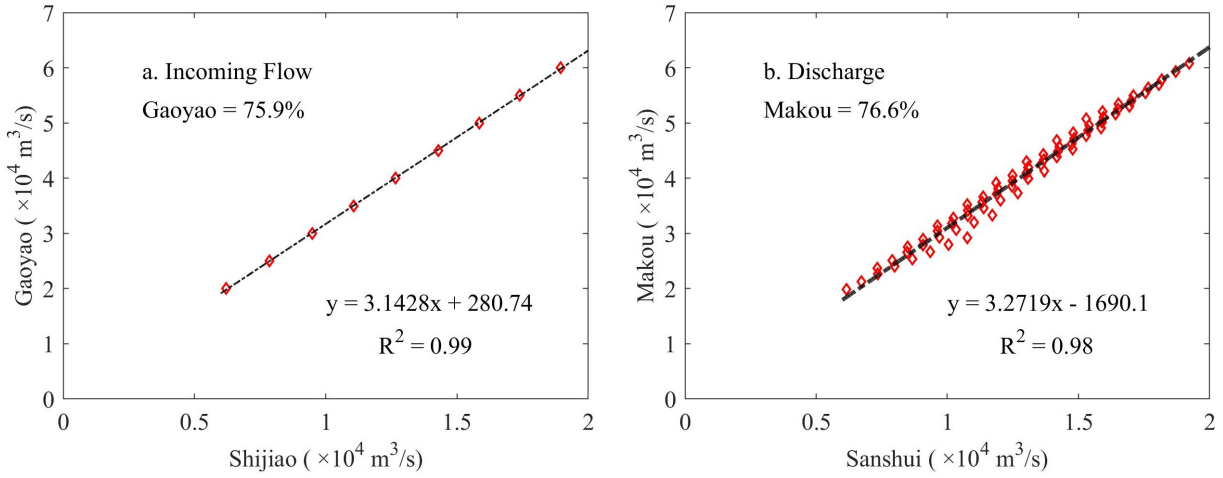

Figure 11. The scatter plot of (a) incoming flow at Gaoyao from West River versus Shijiao from North River when there was no flood diversion, and (b) the discharge at Makou versus Sanshui when various flood diversion occur via the SXJ waterway.

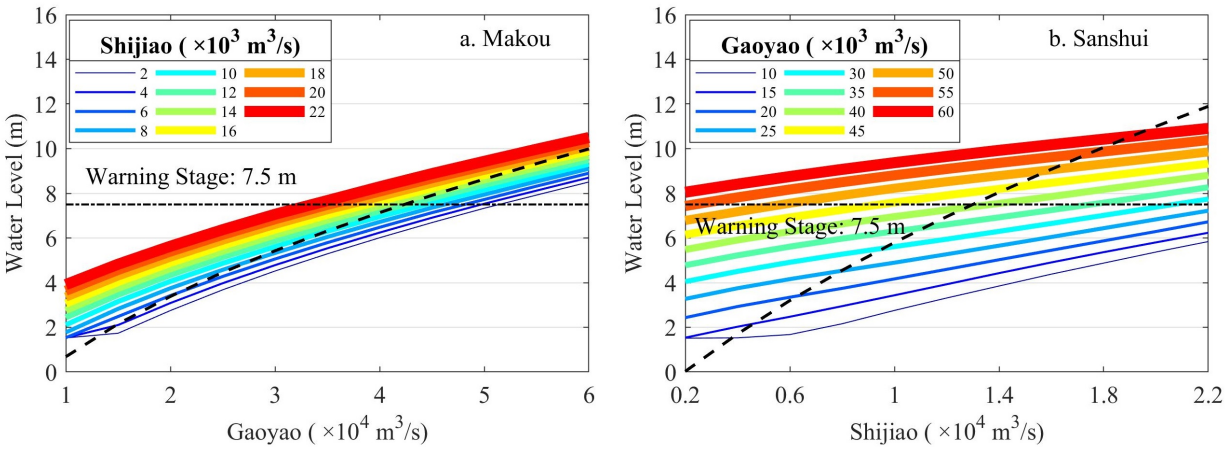

Figure 12. Comparison of water levels at the downstream Makou (a) and Sanshui (b) with and without (dashed line) flood diversion via the SXJ waterway under various incoming flow at Gaoyao from West River and at Shijiao from North River. Below the dashed line, it indicates water level decline at Makou and Sanshui due to flood diversion.

5. Discussions

We discuss the crucial role of the man-made SXJ waterway on flood diversion, on the unstable equilibrium and stabilization of the H-shaped SXJ node, and the diversion influence beyond the SXJ node.

5.1 Evolution from X-shape to H-shape

Over a thousand years ago, the SXJ node was in X-shape with a wide bay and natural low-lying floodplains that flood water could easily exchange between West River and North River, and quickly drain into the estuary (Zeng and Huang, 1982; Ying et al., 1988; Wu, 2018). With aggradation of sediment and human embankment, West River and North River had been separated and are connected by a near 3-km length and 400-m wide waterway at present, forming a unique H-shaped node with double bifurcations and constrained flood water diversion (Liu, 2014). Meanwhile, the downstream river network has been extended seaward and channelized with high levees (Wang et al., 2021). Thus, the man-made SXJ waterway plays a crucial role on flood diversion and mass redistribution for West River, North River, and the downstream river network.

5.2 Flood diversion and equilibrium

The H-shaped SXJ node is usually in unstable equilibrium modulated by flow diversion via the SXJ waterway, which acts like a see-saw driven by the water level difference between its north mouth and west mouth, and is often disrupted by the unbalanced upstream flood waves and the asynchronous tidal force in downstream branches (Zhang et al., 2014; Wu, 2018).

During a single-wave flood, the flood diversion is determined by the relative magnitude of the upstream flood waves from West River and North River (Figure 7). For a single flood occurred in either river basin like the 2005 flood event in the West River basin, the flood wave from the West River compelled the SXJ node into an unstable state, and the near equilibrium before flood was dramatically disrupted by the large water level difference between the north mouth and west mouth in the SXJ waterway (Wu, 2018). Without flood diversion, the maximum water level difference would be up to 4.0 m, which is highly unstable and may cause levee breach or river avulsion, but was reduced to 0.23 m with flood diversion and recovered to near zero or return to equilibrium on July 10, 2005 after flood retreated (Figure 7c & d). The flood water was diverted from West River to North River with a peak rate of -5630 m^3/s, reduced the peak water level at Makou by 0.70 m and increased the peak water level at Sanshui by 3.30 m, making both rivers approach equilibrium (Figure 7c & d).

For a long-term flood event with multiple flood waves occurred in both basins such as in July 2006 and in June 2022 (Figures 8 & 9), the flood diversions in the SXJ waterway were controlled alternatively by the flood waves from West River and North River. There exists a critical incoming flow ratio that poses a similar water level at the west mouth and north mouth, resulting in near equilibrium with little flood diversion (Liu, 2016). Such a critical flow ratio (Gaoyao/[Gaoyao+Shijiao] = 75.9%) was fitted with steady flow simulations using the 121 combinations of incoming flow (Figure 10a & b, Figure 11a), and was slightly larger than that (72.3%) fitted using the incoming flow ratio and diversion flow estimated by a numerical model of the river network (Liu, 2016). When the incoming flow ratio is larger than this critical value, the flood

water will divert from West River to North River; otherwise, the flood diversion reverses direction.

Besides the critical incoming flow ratio, the discharge ratio at the downstream Makou and Sanshui approaches a stable value during individual flood events (Figures 7b-9b) and fluctuates around a critical value for the scenario simulations of 121 incoming flow combinations (Figure 10d) once the discharge rate at Makou is larger than 20 000 m^3/s, or the water level at Makou is higher than 3.0 m (Figure 3a) when the influence of tidal force on flow diversion turns to secondary or even negligible with higher water levels (Liu, 2016). The fitted critical discharge ratios (Makou/[Makou+Sanshui] = 76.6%, ranging from 74.3% to 77.6%) in Figure 10d and Figure 11b are consistent with those observed during the flood events in 2005 (Makou =77.2%), 2006 (Makou =76.8%) and 2022 (Makou =75.9%) (Figures 7b-9b). Such a critical discharge ratio acts like an equilibrium indicator of the SXJ node and is significant for engineering design on flood control and water resource allocation for the downstream waterways and estuary management. In practical calculation of the flood design stage for the downstream waterways, the flood allocation at Makou and Sanshui was estimated using three empirical relations according to the dominated flood in either river basins, resulting in mean discharge ratios at Makou by 75.8%, 74.3%, and 73.7%, respectively (DWR, 2002). Our fitted value is consistent with and confirmed that (75.8%) estimated by the first empirical relation, but still need further investigation especially under the influence of estuary tides and in unsteady flow for scenario simulation considering the flood processes and phase lags in both river basins like three flood events (Figures 7-9).

5.3 Diversion influence beyond the SXJ node

The largest diversion flow (-6930 m^3/s) in the SXJ waterway was observed on July 22, 1996, which reduced the peak water levels in West River at the downstream Makou by 0.96 m and at the upstream Gaoyao by 0.79 m (Li, 1997). This indicated that the flood diversion in the SXJ waterway not only reduced the peak water levels in the downstream, but also reduced the peak water levels in the upstream near the SXJ node since the declined water levels in the downstream increased the water surface slope and flow velocity of flood waves (Li, 1997). The flood diversion from West River to North River not only dramatically increased the peak water level in the downstream at Sanshui by 3.30 m, but also increased the peak water levels in the upstream above Sanshui and at Shijiao, showing strong backwater effect in the lower part of North River.

In addition, the flood diversion in the SXJ waterway is also affected by the tidal levels in the estuary. The modeling results of Liu (2016) suggested that higher tidal levels would reduce the flood discharge ratio at Makou. Since Gaoyao and Shijiao are the upstream boundary stations, Makou and Sanshui are the downstream end of model domain in our model setup, this study did not investigate the influence of flood diversion on the peak flow and water levels in the upstream above the SXJ node, nor examine the estuary tidal influence on the flood diversion via the SXJ waterway and on the discharge ratio at Makou

or Sanshui, although the tidal influence on flood diversion in the SXJ waterway turns secondary as water level is higher than 3.0 m at Makou, or even negligible for a larger magnitude of flood, such as those of 1:5a return period, whose water level at Makou would be higher than 6.5 m. Those issues will be explored in our further studies by setting upper boundary stations and extending the downstream model domain into the estuary.

6 Conclusions

The SXJ node evolved from an X-shape with free water (mass) exchange over a thousand years ago into a unique H-shape that both West River and North River have been separated and connected by the 3-km length and 400-m wide SXJ waterway. The man-made H-shaped node with constrained water exchange created an unstable state due to especially unbalanced flood waves from upstream rivers and the asynchronous tides in the downstream branches, while always approached equilibrium by flow diversion via the SXJ waterway, which acts like a see-saw driven by the water level differences between the north mouth and west mouth.

The Delft3D model is built to simulate the flood diversion and discharge distribution at the SXJ node. Under different incoming flow rates when it is over 20 000 m^3/s at Gaoyao from West River, there exists a critical flow ratio threshold of 75.9% (or 24.1% at Shijiao) that the incoming flow from both rivers poses a similar water level at the west mouth and north mouth, resulting in near equilibrium and little flood diversion via the SXJ waterway. Above the threshold, flood water will divert from West River to North River with a maximum rate of -10700 m^3/s, reducing the peak water level up to 1.48 m at Makou. Below the threshold, flood water will divert from North River to West River with a maximum rate of 11900 m^3/s, reducing the peak water level up to 6.63 m at Sanshui.

The discharge ratio at the downstream Makou and Sanshui approaches a stable value during flood and fluctuates around a critical value of 76.6% (Makou/[Makou+Sanshui]) as the discharge rate at Makou is larger than 20000 m^3/s, or the water level at Makou is higher than 3.0 m when the influence of tidal force on flow diversion becomes secondary, or even negligible with higher water levels. This critical discharge ratio is consistent with those observed during the flood events in 2005 (Makou =77.2%), 2006 (Makou =76.8%) and 2022 (Makou =75.9%), and confirm the empirical relation adopted in calculating the design flood stages along the waterways in the PRD. Such a critical discharge ratio acts like an equilibrium indicator of the SXJ node and is significant for engineering design on flood control and water resource allocation for the downstream waterways and estuary management, but still need further investigation especially under the influence of estuary tides.

Acknowledgments

This study is financially supported by National Key R&D Program of China (2021YFC3001000), National Natural Science Foundation of China (41871085)

and the Innovation Group Project of Southern Marine Science and Engineering Guangdong Laboratory (Zhuhai) (311021004). Authors express their gratitude to the Deft3D model developers, to the Pearl River Hydraulic Research Institute of Pearl River Water Resources Commission of Ministry of Water Resources for offering the river bathymetry, and to the Department Water Resources of Guangdong Province for providing hourly flow and water level data, which were not publicly accessible.

References

Allen, J. I., Somerfield, P. J., & Gilbert, F. J. (2007). Quantifying uncertainty in high-resolution coupled hydrodynamic-ecosystem models. *Journal of Marine Systems*, 64(1-4), 3-14. https://doi.org/10.1016/j.jmarsys.2006.02.010

Bertoldi, W. (2004). River bifurcations. Ph.D. thesis, *Univ. Digli Studi di Trento*, Trento, Italy.

Bolla Pittaluga, M., Repetto, R., & Tubino, M. (2003). Channel bifurcation in braided rivers: Equilibrium configurations and stability. *Water Resources Research*, 39(3). https://doi.org/10.1029/2001WR001112

Buschman, F. A., Hoitink, A., van der Vegt, M., & Hoekstra, P. (2010). Subtidal flow division at a shallow tidal junction. *Water Resources Research*, 46(12). https://doi.org/10.1029/2010WR009266

Deltares (2018). Delft3D-FLOW. User Manual 3.15.57696, *Delft*, Netherlands.

Department of Water Resources (DWR) in Guangdong Province. (2002). Manuals for the design flood stages in the downstream of Xijiang and Beijiang and in the river networks in the Pearl River Delta. Internal document issued by the Department of Water Resources in Guangdong Province, Guangzhou, 2002 at http://slt.gd.gov.cn/.

Ferguson, R. I., Ashmore, P. E., Ashworth, P. J., Paola, C., & Prestegaard, K. L. (1992). Measurements in a braided river chute and lobe: 1. Flow pattern, sediment transport, and channel change. *Water Resources Research*, 28(7), 1877-1886. https://doi.org/10.1029/92WR00700

Ji, X., & Zhang, W. (2019). Tidal influence on the discharge distribution over the Pearl river Delta, China. *Regional Studies in Marine Science*, 31, 100791. https://doi.org/10.1016/j.rsma.2019.100791

Kleinhans, M. G., Wilbers, A., & Ten Brinke, W. (2007). Opposite hysteresis of sand and gravel transport upstream and downstream of a bifurcation during a flood in the River Rhine, the Netherlands. *Netherlands Journal of Geosciences/Geologie en Mijnbouw*, 86(3)

Kleinhans, M. G., Jagers, H., Mosselman, E., & Sloff, C. J. (2008). Bifurcation dynamics and avulsion duration in meandering rivers by one-dimensional and three-dimensional models. *Water Resources Research*, 44(8). https://doi.org/10.1029/2007WR005912

Kleinhans, M. G., Ferguson, R. I., Lane, S. N., & Hardy, R. J. (2013). Splitting rivers at their seams: bifurcations and avulsion. *Earth Surface Processes and Landforms*, 38(1), 47-61. https://doi.org/10.1002/esp.3268

Lesser, G. R., Roelvink, J. V., van Kester, J. T. M., & Stelling, G. S. (2004). Development and validation of a three-dimensional morphological model. *Coastal Engineering*, 51(8-9), 883-915. https://doi.org/10.1016/j.coastaleng.2004.07.014

Li, T. (1997). The role of Sixianjiao in the July 1996 flood. *Guangdong Water Resources and Hydropower*, (01), 22-24 (in Chinese).

Li, Y. (2018). Stage-Discharge Relation Based on "2017.7" Measured Flood in Sixianjiao Channel. *Guangdong Water Resources and Hydropower*, (04), 11-15 (in Chinese).

Liu, F., Xie, R., Luo, X., Yang, L., Cai, H., & Yang, Q. (2019). Stepwise adjustment of deltaic channels in response to human interventions and its hydrological implications for sustainable water managements in the Pearl River Delta, China. *Journal of Hydrology*, 573, 194-206. https://doi.org/10.1016/j.jhydrol.2019.03.063

Liu, J. (2014). Analysis of Functions of Major Nodes in Pearl River Delta River Network. *Pearl River*, 35(6), 48-54 (in Chinese).

Liu, J. (2016). The Pearl River Delta Sixianjiao Channel, Tianhe Node Split Ratio on Law. *Pearl River*, 37(5), 15-20 (in Chinese).

Liu, Q., & Wu, C. (2005). Hydrodynamic Characteristics of Waterway Network of the Pearl River Delta in the 1950's. *Port & Waterway Engineering*, (3), 66-69 (in Chinese).

Liu, X. (2008). Analysis of Flow in Sixianjiao. *Pearl River*, (2), 36-39 (in Chinese).

Luo, X., Zeng, E. Y., Ji, R., & Wang, C. (2007). Effects of in-channel sand excavation on the hydrology of the Pearl River Delta, China. *Journal of Hydrology*, 343(3-4), 230-239. https://doi.org/10.1016/j.jhydrol.2007.06.019

Maréchal, D. (2004). A soil-based approach to rainfall-runoff modelling in ungauged catchments for England and Wales. Ph.D. thesis, *Cranfield Univ.*, Cranfield, U. K.

Nash, J. E., & Sutcliffe, J. V. (1970). River flow forecasting through conceptual models part I—A discussion of principles. *Journal of Hydrology*, 10(3), 282-290. https://doi.org/10.1016/0022-1694(70)90255-6

Pinos, J., & Timbe, L. (2019). Performance assessment of two-dimensional hydraulic models for generation of flood inundation maps in mountain river basins. *Water Science and Engineering*, 12(1), 11-18. https://doi.org/10.1016/j.wse.2019.03.001

Ramamurthy, A. S., Qu, J., & Vo, D. (2007). Numerical and experimental study

of dividing open-channel flows. *Journal of Hydraulic Engineering*, 133(10), 1135-1144. https://doi.org/10.1061/(ASCE)0733-9429(2007)133:10(1135)

Schuurman, F., & Kleinhans, M. G. (2015). Bar dynamics and bifurcation evolution in a modelled braided sand-bed river. *Earth Surface Processes and Landforms*, 40(10), 1318-1333. https://doi.org/10.1002/esp.3722

Shen, J. (1989). Calculation of the mean daily discharge through the Sixianjiao waterway in low-water season. *Tropical Geography*, 09(02), 143-149 (in Chinese).

Wang, X., Huang, J., & Xu, H. (2015). Study of Hydrological Characteristics in Sixianjiao Reach. *Guangdong Water Resources and Hydropower*, (11), 26-30 (in Chinese).

Wang, X., Guo, Y., & Ren, J. (2021). The Coupling Effect of Flood Discharge and Storm Surge on Extreme Flood Stages: A Case Study in the Pearl River Delta, South China. *International Journal of Disaster Risk Science*, 12(4), 1-15. https://doi.org/10.1007/s13753-021-00355-5

Wang, Z. B., De Vries, M., Fokkink, R. J., & Langerak, A. (1995). Stability of river bifurcations in 1D morphodynamic models. *Journal of Hydraulic Research*, 33(6), 739-750. https://doi.org/10.1080/00221689509498549

Wu, C. (2018). A preliminary study on the phenomenological relation between morphodynamic equilibrium and geomorphic information entropy in the evolution of the Zhujiang River Delta. *Haiyang Xuebao*, 40(07), 22-37 (in Chinese)

Wu, C., & Wei, X. (2021). From drowned valley to delta: Discrimination and analysis on issues of the formation and evolution of the Zhujiang River Delta. *Haiyang Xuebao*, 43(1), 1-26 (in Chinese)

Wu, Y., Zhang, W., Zhu, Y., Zheng, J., Ji, X., & He, Y., et al. (2018). Intratidal division of flow and suspended sediment at the first order junction of the Pearl River Network. *Estuarine, Coastal and Shelf Science*, 209, 169-182. https://doi.org/10.1016/j.ecss.2018.05.030

Xie, P., Tang, Y., Chen, G., & Li, C. (2010). Variation analysis of hydrological and sediment series in North River and West River Delta: case study of Makou Station and Sanshui Station. *Journal of Sediment Research*, (05), 26-31 (in Chinese).

Ying, Z., Chen, Z., & So, C. L. (1988). Formation and Evolution of the X-Shape waterways by Sixianjiao Channel. *Sun Yat-sen University Forum*, (02), 8-14 (in Chinese).

Zeng, Z., & Huang, S. (1982). Study on the historical geomorphology of the convergence area of branching channels in the Pearl River Delta, taking the development of a sandbar in Sixianjiao as an example. *Pearl River*, (04), 25-29 (in Chinese).

Zhang, W., Du, J., Zheng, J., Wei, X., & Zhu, Y. (2014). Redistribution of the suspended sediment at the apex bifurcation in the Pearl

River Network, South China. *Journal of Coastal Research*, 30(1), 170-182. https://doi.org/10.2112/JCOASTRES-D-13-00002.1

Zhang, W., Cao, Y., Zhu, Y., Wu, Y., Ji, X., & He, Y., et al. (2017). Flood frequency analysis for alterations of extreme maximum water levels in the Pearl River Delta. *Ocean Engineering*, 129, 117-132. https://doi.org/10.1016/j.oceaneng.2016.11.013

Zhang, W., Cao, Y., Zhu, Y., Zheng, J., Ji, X., & Xu, Y., et al. (2018). Unravelling the causes of tidal asymmetry in deltas. *Journal of Hydrology*, 564, 588-604. https://doi.org/10.1016/j.jhydrol.2018.07.023